Colloids and Surfaces A: Physicochemical and Engineering Aspects 659 (2023) 130742

Contents lists available at ScienceDirect

Colloids and Surfaces A: Physicochemical and Engineering Aspects

journal homepage: www.elsevier.com/locate/colsurfa

Fecalphobic oil-coated femtosecond-laser-processed PTFE surface

Yu Liu [a,c], Gan Yuan [a,c], Fei Xie [a,c], Yang An [a], Jianwen Sun [b,c], Ning Zhao [b,c], Yongbo Deng [b,c], Longnan Li [a], Subhash C. Singh [d], Chi-Vinh Ngo [a,*], Wei Li [a,c,*], Chunlei Guo [d,**]

[a] GPL Photonics Laboratory, State Key Laboratory of Applied Optics, Changchun Institute of Optics, Fine Mechanics and Physics, Chinese Academy of Sciences, Changchun, Jilin 130033, China
[b] State Key Laboratory of Applied Optics, Changchun Institute of Optics, Fine Mechanics and Physics, Chinese Academy of Sciences, Changchun, Jilin 130033, China
[c] University of Chinese Academy of Science, Beijing 100049, China
[d] The Institute of Optics, University of Rochester, Rochester, NY 14637, USA

HIGHLIGHT

- The fecalphobic surface fabricated by silicone-oil coated laser-ablated PTFE was investigated.
- A toilet design was optimized to a urine-feces separation and trap door component.
- Fecal simulant slides off the fecalphobic surface approximately 3–26 times faster than off an untreated one.
- The fecalphobic surface can make the toilet use less water even no water.
- Water cost for cleaning the trapdoor fecalphobic surface is at least 3 times less than other surfaces.

GRAPHICAL ABSTRACT

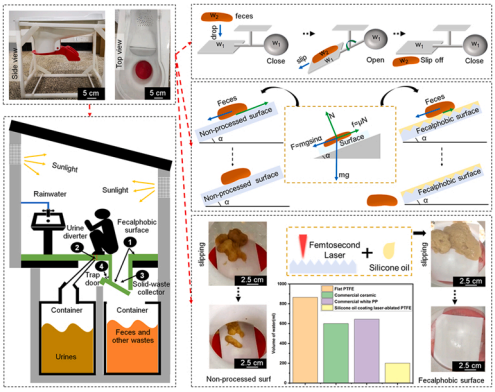

ARTICLE INFO

Keywords:
Urine-feces separation
Fecalphobic trapdoor
Polytetrafluoroethylene
Femtosecond laser ablation
Pit-latrine toilet

ABSTRACT

Water, sanitation, and hygiene (WASH) investments have become crucial not only to prevent and recover from pandemics and local outbreaks but also to prevent the spread of antimicrobial resistance. However, over 2 billion people worldwide still have access to even poor sanitation, which devastates public health and social and economic development. In addition, inadequate sanitation can cause contamination to drinking water sources where exist insufficient protection, exacerbating clean water scarcity. Here, we introduce a femtosecond laser processing technology combined with silicone oil coating to prepare a slippery surface that can repel feces, named the fecalphobic surface. Compared to a flat surface, the fecalphobic surface requires only a quarter amount of water (on average) or even no water to remove sticky viscoelastic solid-like fecal simulants. Besides, various liquids will slide off this surface. Moreover, the simulant slides off the fecalphobic surface much faster than off an untreated one, approximately 3–26 times faster depending on their weight. The mechanism of the fast sliding of

* Corresponding author at: GPL Photonics Laboratory, State Key Laboratory of Applied Optics, Changchun Institute of Optics, Fine Mechanics and Physics, Chinese Academy of Sciences, Changchun, Jilin 130033, China.
** Corresponding author.
E-mail addresses: chivinh@ciomp.ac.cn (C.-V. Ngo), weili1@ciomp.ac.cn (W. Li), guo@optics.rochester.edu (C. Guo).

https://doi.org/10.1016/j.colsurfa.2022.130742
Received 20 October 2022; Received in revised form 26 November 2022; Accepted 30 November 2022
Available online 5 December 2022

fecal simulants is explained. Moreover, the fecalphobic surface is installed on a latrine prototype that integrates an automatic trap door and a urine-feces separator for improved sanitation solution.

1. Introduction

Sustainable Development Goal 6 (SDG6) commits all people to have access to adequate and equitable sanitation and hygiene as well as ending open defecation by 2030 [1]. Although sanitation coverage rates exceed 95 % in developed countries, many countries are not on track to achieving the millennium development goals for sanitation that coverage is broader than 75 % by WHO and UNICEF in 2014 [2]. Despite the fact that the situation has improved since 2019, over 2 billion people still lack basic sanitation, and nearly half of the world's population, approximately 45 %, do not have access to safely managed sanitation services [1,3]. About one out of eight people worldwide practiced open defecation in 2015, showing the worse result in developing countries [4]. As reported in 2020, about 494 million people still practice open defecation [3]. Open defecation can cause a variety of pathogenic bacteria or viruses (such as malaria, and parasites) to spread widely, making the population more susceptible to pathogen infection, adversely affecting human health, especially children. In developing countries, fecal-oral contamination is the root cause of more than 50 % of children's deaths before 2011 [2,5]. Until 2020, there are still nearly 698 million school-age children who lack basic sanitation services in school. Simultaneously, poor sanitation and fecal management also negatively impact the environment by polluting water, soil, and food sources [6]. Many countries have promoted the use of toilets to increase the utilization rate of toilets and reduce disease problems caused by open defecation [7–9]. Based on the current statistic mentioned above, the pace of development in sanitation must quadruple in order to meet the 2030 SDG targets. However, traditional toilets, relying on tap water, extensive sewer networks, and expensive treatment systems are costly to build and cannot meet the needs of popular hygiene [10], slowing down the SDG's commitments. To address the problem, more facile and innovative non-sewered toilet systems should be developed, particularly in areas where water is scarce, or the economy is underdeveloped.

Apart from sanitation, clean water is also a significant challenge in the WASH sector. Until now, only 0.5 % of the earth's water content can be sued for daily life, causing water scarcity in many regions [11,12]. For example, India has one-seventh of the global population and is predicted to confront acute water constraints [4,9]. Furthermore, around 30 % of people lack clean water sources for fundamental sanitation needs worldwide. Researchers estimate that about 850,000 people die each year due to a lack of access to safe drinking water, sanitation, and hygiene and that almost two-thirds of the world's population experience severe water shortages for at least one month each year [4,9,13]. However, conventional toilets use 6 – 12 liters of freshwater per flush, which may increase the pure water shortage [14]. Wastewater such as grey water, which can be converted into drinking water, may be employed in conventional toilets to preserve freshwater, the newly created large amount of black water after flushing with freshwater or grey water will require more effort, complex costly processes, and extra energy to be purified into grey water or even drinkable water. On the other hand, providing insufficient flushing water amount can cause the stick of human feces and urine on the toilet surface, resulting in foul odors and possible transmission of many infectious diseases. Significantly, in the countries where water is scarce, current sanitary treatment methods or flush toilet systems that consume much water are not applicable. Multiple studies of toilets have been conducted. Most research works focus on separating feces from urine, and the post-treatment of human wastes [13,15,16], while some approaches have been developed to employ wastewater recycling [13,17] or alternative water sources [18]. However, there are almost no studies solely on reducing water use. Therefore, the invention of toilets that use less or even no water remains a challenge.

Nowadays, superhydrophobic surfaces are wildly applied in anti-corrosion [19,20], anit-icing [21,22], oil-water separation [23,24], water positioning [25], water/bubbles transportation [26–28] anti-bacterial [29,30] and self-cleaning [31,32]. Researches show that low surface energy and micro-nano structure formation are the main factors in achieving superhydrophobic surfaces [33]. However, the air layer formed by micro-nano structures is weak and easily destroyed by higher pressure [34], limiting the applications of superhydrophobic surfaces.

Recently, there have been some studies on Slippery Liquid Infused Porous Surface (SLIPS) by combining femtosecond laser processing, silane, and lubricant coating, which makes up for the lack of superhydrophobic surface [35,36]. For example, Yong et al. [34]. have prepared a slippery Polyamide6 (PA6) surface with self-healing property by laser fabrication combined with fluoroalkylsilane treatment and then the superhydrophobic PA6 coating with silicone oil. Lubricant is known to reduce solid-solid friction [37]. As a common lubricant, silicone oil has a wide range of applications in industry, agriculture, and medicine due to its nonvolatility and environmentally friendly property [38,39]. Additionally, laser processing can create micro-nano structures, increasing lubricant storage and allowing the sample to be used for a more extended period [34,40,41]. However, all current studies are only focused on applications with liquid-repellent surfaces. There still lacks research on the slippery performance of sticky viscoelastic solids like human feces and fecal simulants. Only Wong's group [42] applied a two-step spray-coating on a glass substrate to produce an anti-fecal adhesion surface. However, the glass substrate is not easy to use for practical applications due to its brittleness, and the research intends to focus on modern flush toilets, which are hard to be applied in water-scarce areas.

Herein, a femtosecond laser surface processing combined with silicone oil coating on Polytetrafluoroethylene (PTFE) was employed to produce fecalphobic surfaces. The fabricated surfaces were investigated for liquid repellency to sticky viscoelastic solid repellency. All the samples showed high performance in liquid repellency, enabling a self-cleaning ability from unwanted liquids on toilet surfaces. Moreover, the fecalphobic surfaces require less water (approximately half of the necessary amount) or even no water to remove the fecal simulant. Additionally, the simulant slides much faster on the fecalphobic surface, 3–26 times depending on the simulant's weight, minimizing bacteria growth on the toilet surface under the ambient air. The sliding mechanism of the fecalphobic surface was also explained. Furthermore, such surfaces were applied in our urine-feces separation pit-latrine prototype to test fecalphobic performances. The toilet could save water and energy. These results suggest a toilet model for better sanitation and hygiene when applied to water-scarce countries, thereby improving safety and sanitation of toilet use.

2. Experimental section

2.1. Materials

PTFE large plates ($30 \times 30 \times 0.2$ cm^3) were purchased by Aladdin biochemical technology co. LTD. Silicone oil (A.R) was provided by the State-owned Beijing Yongding Chemical Plant. Ethanol (A.R) was obtained from the Sinopharm Chemical Reagent Co., Ltd. The fecal simulant components were purchased from different companies. In detail, yeast extract and cellulose were provided by Wuhan Qinghui Biotechnology Co., LTD, and Hebei Baiyou Biotechnology Co., LTD, respectively. $CaCl_2 \bullet 2\ H_2O$ was bought from Shanghai Hushan Chemical Co.,

LTD. NaCl and KCl were both purchased from Beijing Chemical Works. Oleic acid was purchased from Wuxi Yatai United Chemical Co. LTD. The miso paste and the baker yeast were bought from a Chinese market. Polypropylene (PP) plates were used to produce the toilet frame and components.

2.2. Experiment process

2.2.1. Fabrication of fecalphobic surface

The PTFE large plates were cut into many small pieces with different sizes (1.5 × 1.5 cm^2; 5 × 5 cm^2; 10 × 17 cm^2). After cutting, the impurities on PTFE surfaces were removed using ultrasound cleaning with deionized water (DI water) for 20 mins and then with ethanol for 20 mins. After ultrasonic cleaning, nitrogen was used to dry the sample.

After the ultrasonic cleaning, a high-power femtosecond laser (pharos-light conversion, maximum power of 20 W; maximum energy of 400 μJ) and a galvanometer scanner were employed to fabricate micro-nano structures on the PTFE surfaces (Fig. 1a). In the laser ablation process, laser powers, repetition rates, step sizes, and scanning speeds were changed to control the surface morphologies. We could get samples with different depths and widths with these parameters. The ratios between the widths and the depths (W/D) were also studied. After that, the final six parameters were chosen and presented in Table S1, which were named P1 to P6.

After the laser processing, the silicone oil was coated onto the sample's surface (Fig. 1b). To ensure that the oil was already covered in all the grooves, the oil was added with a small amount to the surfaces and added three times. The thickness of the film was controlled by the volume of the surface structures. The total volume of the oil was a little bit more than the total capacity of the sample grooves. After coating, samples were named T1 to T6, which related to the samples P1 to P6. Moreover, after coating with silicone oil, the non-processed PTFE surface (P0) was called T0.

2.2.2. Preparation of fecal simulant

The solid compositions of feces consist mainly of proteins, fats, fibers, bacteria, inorganic substances, and carbohydrates. Moreover, in the compositions, the percentage of live and dead bacteria is 25–54 % of the actual feces' dry weight. Besides, the average moisture content of natural manure was approximately 75 %, fluctuating between 63 % and 86 % [43]. One of the main factors influencing moisture variation is the difference in water absorption, which is caused by the difference in cellulose content in manure. After studying actual feces compositions, we found that feces' compositions, nature, and physical properties are influenced by many factors, such as geographical differences, differences in food and water intake, and differences in physical condition [44]. Moreover, the presence of many microorganisms in feces like E. coli can affect the preservation of feces. In case of improper handling, the health of the experimenter can be seriously affected. Therefore, we did not choose human stools at the beginning of the experiments but used fecal simulants instead. This can prolong the testing time on the samples and ensure the health of the experimenters. Moreover, we can control the physical and chemical properties of the simulants by controlling the compositions of the substances in the simulants, thus reducing experimental errors.

After investigating the different compositions of fecal simulant, we referred to a fecal simulant composition in Penn's manuscript, and the SB80 type was finally chosen [43]. The compositions and the purpose of the SB80 are presented in Table S2. The preparation process was as follows: First, we mixed the dry powder (Yeast extract; Baker's yeast; Cellulose; Psyllium; NaCl; KCl; $CaCl_2 \bullet 2\ H_2O$) together; After mixing the powder, we added the oleic acid and mixed thoroughly. Then, the miso paste was added into the mixture, and completely mixed. Finally, we weighed the water and slowly added it into the bottle with stirring at the same time. After mixing all the materials, we covered the bottle and then put it at room temperature for at least 1.5 h to make the mixture become a fecal simulant, which exists a similar property to actual wastes but is not harmful to users. The fecal simulant states of all processes are shown in Fig. S1.

2.2.3. Fabrication of a new pit-latrine toilet

Original latrine toilet designs require a large amount of water to wash the feces and urine together. In this study, we developed a new latrine toilet type which is integrated a urine-feces separator and a fecal-phobic trap door, which could automatically open and close (Fig. 1c). When someone uses this toilet, the urine will almost go into the urine separation part, and the feces will go into the feces separation part. And our fecal-phobic surface was attached to the trap door, which could make the simulant slides down the surface. Due to this requirement, a 3D model was produced. Referring to this model, a simple prototype without the trapdoor was made by a conventional thermoplastic molding process. A trap door and a urine diverter component were then installed in the molded prototype. The final obtained PP prototype in this study was optimized from a typical pit-toilet model with urine separation holes and a trapdoor component.

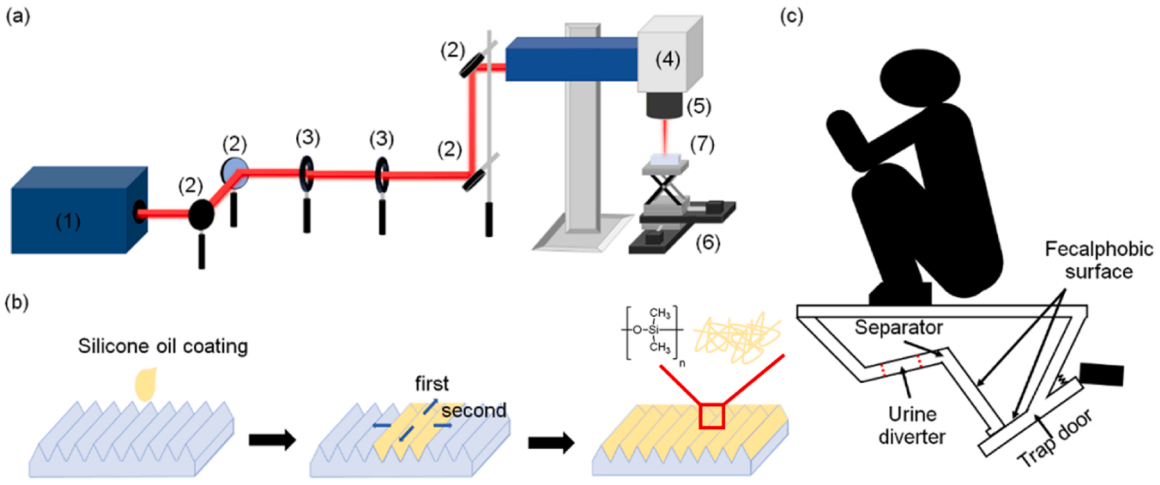

Fig. 1. Fabrication of fecalphobic surface and new pit latrine toilet. (a) Femtosecond laser system: (1) Femtosecond laser source, (2) Optical mirror, (3) Iris, (4) Galvanometer scanner head, (5) F-theta lens, (6) 3D translation stage, and (7) sample . (b) The silicone oil coating and diffusion process. (c) Schematic describing the design strategy of the new pit latrine toilet.

2.3. Characterization process

2.3.1. The surface morphology and wettability test

In order to characterize and analyze the samples, we tested the scanning electron microscope (SEM) (ProX800–07334, Phenom World), and 3D confocal UV scanning laser microscope (KEYENCE, VK-X 1000) to check the surface morphology. The energy dispersive spectrometer (EDS) and Fourier Transform infrared spectroscopy (FTIR) was used to characterize elements and chemical bonding. The thickness of the oil layer was calculated based on the weight change of the sample before and after silicone oil coating. To investigate the wettability of the samples, we tested the samples' water contact angles (WCAs) and water sliding angles (WSAs) before and after the silicone oil coating. After measuring the WCAs, the sliding property of the sample before and after coating silicone oil was also tested. The sample was placed on a 20° turntable. Then the dyed deionized water (DI water) was dropped onto the sample's surface. The process of how the dyed DI water droplets slid on the sample's surface was observed. What's more, a high-speed camera was employed to check the impacts of 10 μl water droplets on the surfaces.

2.3.2. The fecal simulant characterization and fecal repellence property test

After getting the proper fecal simulant, the fecal phobic repellence test was carried out. A sample of size 5 × 5 cm^2 was placed on a platform with an inclination angle of 30°. A configured fecal mock-up with a mass of 5 ± 0.5 g was thrown downwards. The height of each throw was kept at the same height level, approximately 7 cm.

In the subsequent tests, a large sample of 10 × 17 cm^2 with a laser processing area of 10 × 10 cm^2 was prepared based on the best-obtained result on the small-size samples. The large sample was fixed on our custom-built toilet model to test how well the fecal-phobic surface works in a close to actual situation. According to research, studies have found that the wet feces weight of each person's daily bowel movements is in the range of 70–520 g [2].

Therefore, we put the prepared fecal simulant in a sealed bag and controlled the weight to 150 ± 5 g. Although the weight was not too heavy, the trapdoor could be automatically smoothly opened when dropping the fecal simulant. During the test, the opening part of the sealed bag was controlled at the same size, and the throw height (15 cm) was also maintained at the same value. The adhesion amount of the fecal simulant on the surface of the final sample and the water cost for cleaning the sample surface can be used to determine the sample's repel performance. Additionally, the friction test was also carried out.

3. Result and discussion

3.1. Surface morphology and chemistry

Femtosecond laser pulses interacted with PTFE by the two mechanisms of laser-induced material removal and polymer gasification, leading to porous structures [45]. It could conclude that the higher the laser energy, the higher the repetition rate, and the slower the scanning speed causes the higher thermal effect. Due to the melting effect, the laser processing area was smoother, and on the contrary, the sample surface was more porous (Figures 2a1, a2, b1, b2, and S2). After coating, the silicone oil covered all the sample surfaces because the depths of the grooves could not be measured (Figures 2a3, b3, and S2). Moreover, the ratios between the grooves' width and depth (W/D) were calculated as shown in Table S3.

A stable lubricating surface has two requirements: (1) Lubricant completely infiltrates the solid surface; (2) Lubricant and test liquid must be immiscible [46]. Oil-film stability was characterized by separation parameter (S) and separation pressure (Π(e)) [42,47,48]. S_{ls} is the separation parameter of lubricant diffusing from the solid surface in the presence of air. S_{lsf} means the separation coefficient of lubricant diffusing on the solid surface in the presence of non-mixed droplets. The separation parameter is expressed as Eqs. (1), (2):

$$S_{ls} = \sigma_s - (\sigma_{ls} + \sigma_l) = 2\sqrt{\sigma_s^{LW}\sigma_l^{LW}} + 2\sqrt{\sigma_l^{+}\sigma_s^{-}} + 2\sqrt{\sigma_s^{+}\sigma_l^{-}} - 2\sigma_l^{LW} - 4\sqrt{\sigma_l^{+}\sigma_l^{-}} \quad (1)$$

$$S_{lsf} = \sigma_{sf} - (\sigma_{ls} + \sigma_{lf}) = 2\sqrt{\sigma_s^{LW}\sigma_l^{LW}} + 2\sqrt{\sigma_f^{LW}\sigma_l^{LW}} + 2\sqrt{\sigma_l^{+}\sigma_s^{-}} + 2\sqrt{\sigma_s^{+}\sigma_l^{-}} + 2\sqrt{\sigma_l^{+}\sigma_f^{-}} + 2\sqrt{\sigma_f^{+}\sigma_l^{-}} - 2\sqrt{\sigma_f^{LW}\sigma_s^{LW}} - 2\sqrt{\sigma_s^{+}\sigma_f^{-}} - 2\sqrt{\sigma_f^{+}\sigma_s^{-}} - 4\sqrt{\sigma_l^{+}\sigma_l^{-}} - 2\sigma_l^{LW} \quad (2)$$

where σ_s, σ_{ls}, σ_l, $\sigma_{sf}$and $\sigma_{lf}$are interfacial tensions of solid–air, liquid–solid,

liquid–air, solid–foreign fluid, and liquid–foreign fluid interfaces. σ^{LW} presents Lifshitz-van der Wass component of interfacial tension; $\sigma^{+}$and σ^{-} indicate the interfacial tension of the acid term and base term polar components, respectively.

Disjoining pressure of silicone oil film can be expressed as Eq. (3):

$$\Pi(e) = A/6\pi e^3 \quad (3)$$

Where e is oil film height, and A is the Hamaker constant expressed as Eq. (4):

$$A = \frac{3}{4}KT\left(\frac{\varepsilon_s - \varepsilon_l}{\varepsilon_s + \varepsilon_l}\right)\left(\frac{\varepsilon_f - \varepsilon_l}{\varepsilon_f + \varepsilon_l}\right) + \frac{3h\nu_e}{8\sqrt{2}} \frac{\left(n_s^2 - n_l^2\right)\left(n_f^2 - n_l^2\right)}{\left(n_s^2 + n_l^2\right)^{1/2}\left(n_f^2 + n_l^2\right)^{1/2}\left[\left(n_s^2 + n_l^2\right)^{1/2} + \left(n_f^2 + n_l^2\right)^{1/2}\right]} \quad (4)$$

where K means Boltzmann constant; T is absolute temperature; h is Planck's constant; v_e equals 2.9 × 10^{15} s^{-1}, means plasma frequency of free electron gas; while $n_{s/l/f}$ and $\varepsilon_{s/l/f}$ are refractive indices and dielectric constants of solid, liquid, and foreign liquid of interest (air or water), respectively. The oil-coated thickness and surface tension are provided (Table S4, S5[42,47,49]).

S_{sl}/S_{slf} (f = air) < 0 meant that silicone oil would not separate easily on sample P0 (Table 1). After laser processing, the grooves made silicone oil easier to spread over the surface by capillary force and form a more stable film [50].

Before and after laser processing, F content both reached about 95 %, while C content accounted for about 5 %, and dominant characteristic peaks of samples appeared at 1200 cm^{-1} as the asymmetric stretching vibration of C-F, and 1140 cm^{-1} as the symmetric stretching vibration of C-F (Fig. 2c, d). The obtained results showed that the chemical composition of PTFE did not change after laser processing, indicating excellent stabilities of PTFE.

3.2. Liquid repellency

Sample P0 is inherently hydrophobic, with a contact angle (CA) of

Table 1
the S and A results of the solid-lubricant-foreign liquid status.

	1	2	3
Solid	PTFE	PTFE	PTFE
Lubricant	silicone oil	silicone oil	silicone oil
Foreign fluid	–	air	water
ε_s	2.1	2.1	2.1
n_s	1.359	1.359	1.359
ε_l	2.8	2.8	2.8
n_l	1.41	1.41	1.41
ε_f	–	1.00054	80.00000
n_f	–	1.00	1.33
S	-818.0500	-818.0500	0.0208
A	–	5.91 × 10^{-21}	6.55 × 10^{-22}

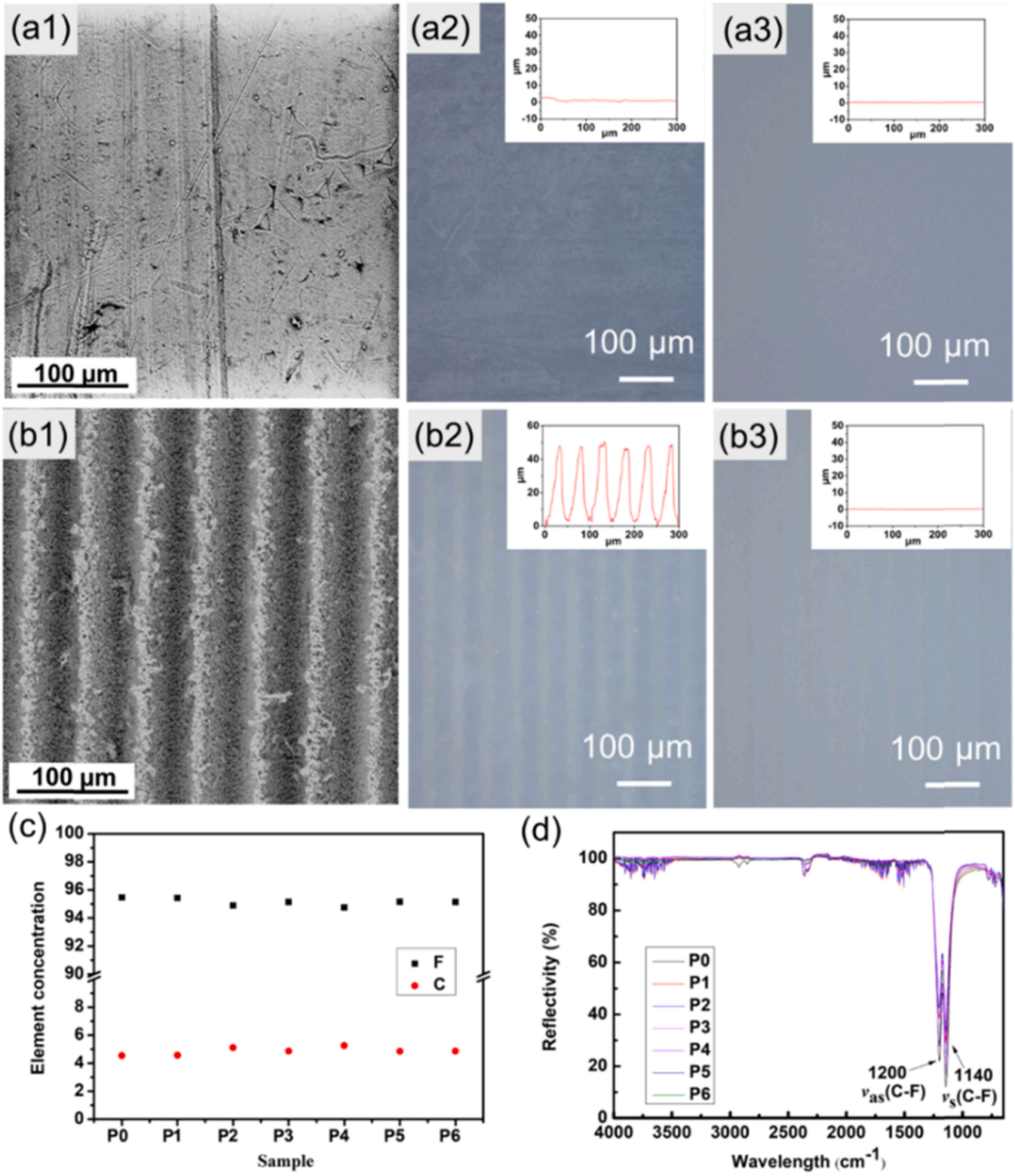

Fig. 2. Surface morphology and structure characterization. (a1, b1) SEM images of non-processed PTFE (P0) and laser-ablated PTFE (P3), respectively; (a2, b2, a3, b3) Confocal microscope images of non-processed PTFE (P0), laser-ablated PTFE (P3), oil-coated non-processed PTFE (T0) and silicone oil-coating laser-ablated PTFE (T3), respectively; The inserted images at the right corner of (a2, a3, b2, b3) are surface profiles of the samples P0, P3, T0, and T3 with the scanning line of the 3D confocal microscope measurement in the horizontal direction. (c, d) EDS and FTIR spectra results of PTFE surfaces before and after femtosecond laser processing (P0–P6).

100°, due to the appearance of the fluorine group. After laser processing, the micro-nano structure formation made PTFE change from hydrophobicity to superhydrophobicity, which is caused by an air-layer formation and low surface energy, reducing the adhesion between samples and droplets. The CAs were greater than 155°, and sliding angles (SAs) were smaller than 10° (Fig. 3a). Moreover, water droplets

bounced off the laser-ablated PTFE while adhering to sample P0 without sliding off (Video S1). Various liquids on sample P0 were hemispherical, but showed spherical shapes on samples P1–P6 (Fig. S3 a1–g1) suited to the Cassie-Baxter model [51].

Supplementary material related to this article can be found online at doi:10.1016/j.colsurfa.2022.130742.

Silicone oil coating on non-processed PTFE showed an angle of 36°, so it could spread on the laser-ablated surface by Wenzel theory [52]. After the silicone oil coating, CAs of all the samples tended to become the same which showed a range of 80–90°, and T1–T6′s SAs were less than 5° (Fig. 3b). Water droplets on samples P0 and P3 showed clear boundaries with the air, but were unclear on sample T3 (Figure 3c1–e1) because the silicone oil layer wrapped them. Moreover, various liquids on samples T0–T6 were also covered in silicone oil and separated on the surfaces (Fig. S3a2–g2). Therefore, water wrapped in silicone oil slowly slid off the surfaces instead of bouncing off the surface (Video S1). In addition, a droplet impact test, followed by the reference [53], was performed on the 20°-tilted surface T3. The water droplets with a 7 μl volume were continuously dropped on the sample at the height of 3 cm. They slid to the bottom with a velocity, approximately 0.99 mm/s. The speed maintained little change with the repetition of up to 800 times.

The result of S_{slf} (f = water) > 0, and A > 0 indicated that the oil layer was stable (Table 1). The droplets on silicone oil coating non-processed PTFE were stable when combined with the calculation and measurement results. Surface wettability could be a primary factor influencing the water droplet impact on the surface [54]. When the water droplet fell on the P0 surface, it started to separate and wholly separated at 5.4 ms, then tended to bounce off but still attached to the surface (Fig. 3f). However, on the P3 surface, the droplet entirely became a pancake shape at 4.6 ms, and because of the lower adhesion [55], it completely bounced off the surface at 15.6 ms (Fig. 3g). The colors of the pancakes on samples P0 and P3 are transparent, representing the color of the water. The color of the pancake on sample T3 is translucent because the silicone oil layer wrapped the water droplet, and the color affects by the appearance color of silicone oil (Fig. S4). Additionally, on the T3 surface, the droplet separated at 2.6 ms, and the oil layer inhibited the rebound of water droplets [56] (Fig. 3h), but partial bouncing may happen (Fig. S4). The oil layer wrapped water droplets, so they were separated on silicone oil coating PTFE more quickly into a pancake shape [57]. Moreover, the oil layer interface was softer and

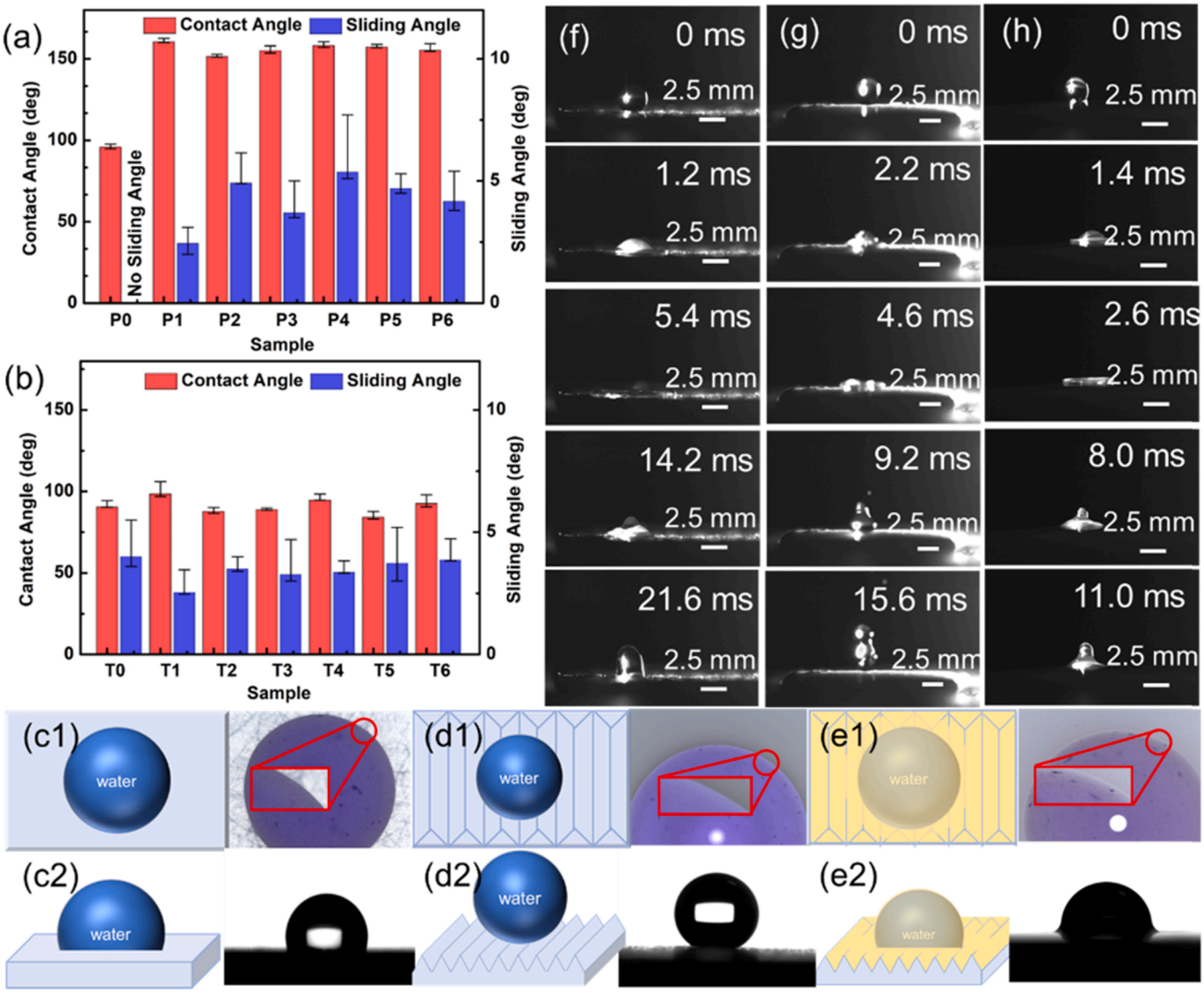

Fig. 3. Liquid repellency of flat PTFE, superhydrophobic PTFE, and slippery fecalphobic PTFE. CAs and SAs of non-processed and laser-ablated PTFE before (a) and after silicone oil coating (b); Observations of water droplets on the surface P0, P3, and T3 were performed with the top view (c1–e1) and side view (c2–e2), respectively. The red circles zoom in on the boundaries of the water droplets. (f–h) captured images of the water drop impact on samples P0, P3, and T3, respectively; The bouncing properties showed apparent differences due to the surface adhesion; Silicone oil coating made the surface have a shorter separation time.

more mobile than the solid surface. So the droplet impact dynamics on various surfaces would be totally different, which showed a distinct separation and bouncing time [56].

3.3. Solid repellency

Silicone oil coating laser-ablated PTFE showed better bonding stability than Silicone oil-coating non-processed ones (Fig. S5). The oil layer on non-processed PTFE was unstable and shrunk over time to expose the bare surface, which was the same agreement as our theoretical calculation. After 7 testing times, fecal simulant was stuck to this surface, while Silicone oil coating laser-ablated PTFE still showed excellent fecalphobicity.

Samples P0, P3, and T3 were examined with 5 ± 0.5 g of fecal simulant (Video S2). On surface P0, when the simulant was dropped, it slid off the surface in 26 s, leaving a small amount of the simulant adhered to the sample surface (Fig. 4a). The simulant stuck seriously to the surface P3 but slid off from surface T3 with the aid of the silicone oil-coated layer, only in 1 s (Fig. 4b, c). Therefore, the simulants could easily slide out of the fecalphobic surfaces in a short time.

Supplementary material related to this article can be found online at doi:10.1016/j.colsurfa.2022.130742.

The surfaces were observed after testing with the simulant (Figs. S6, S7). The laser-ablated PTFE surfaces showed the worst results because

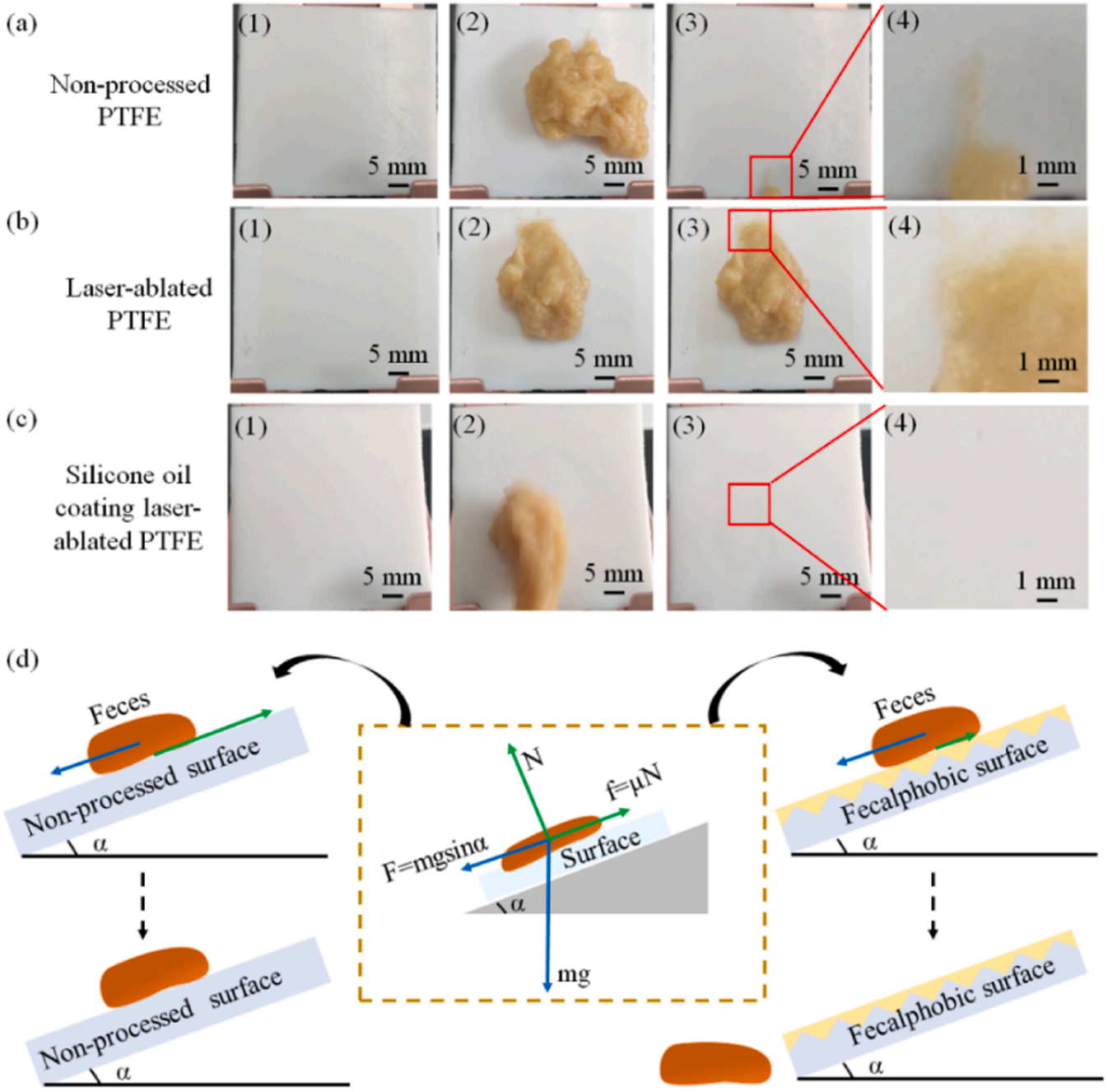

Fig. 4. Sticky viscoelastic solid repellency test on the small-size samples. (a) non-processed PTFE (P0); (b) laser-ablated PTFE (P3); (c) silicone oil-coating laser-ablated PTFE (T3). 5 ± 0.5 g of fecal simulant was dropped to the surfaces at the same height (7 cm) to check the fecalphobicity. The laser-ablated PTFE surface stuck the most amount of fecal simulant while the silicone oil coating laser-ablated PTFE surface repelled the simulant; (d) The Schematic of the force of the fecal stimulant on non-processed PTFE and oil-coated laser-ablated PTFE.

the air layer was destroyed by the strong impact of the fecal simulant, resulting in the attachment of the simulant to most of the surface. The roughness of the laser-ablated PTFE surface causes large adhesion areas to the simulant. The fecal simulant at the small weight (5 ± 0.5 g) could slide off the non-processed PTFE but maintain its small amount of the components. The best result was silicone oil coating laser-ablated PTFE. Silicone oil was stored in the micro-nano grooves and covered the air layer, reducing the adhesion between the fecal simulant and the surface. The surface tension of the fecal simulant was predicted by the surface tension of the water and the silicone oil. There was 70 % water in the fecal simulant, and the surface tension of the fecal simulant must be lower than 72.0 $mN{\cdot}m^{-1}$. Moreover, for the contact and absorption with the silicone oil, the minimum surface tension of the fecal simulant was 20.7 $mN{\cdot}m^{-1}$. Due to this range of the fecal simulant, the S could be calculated by these ranges. The result of the S was larger than 0, indicating the fecal simulant on the surface after oil coating would not touch the structure, and with the help of the silicone oil, the simulant can be easier to slide off the surface. So, when the fecal simulant fell on the surface of the silicone oil coating laser-ablated PTFE, the simulant would not directly touch the micro-nano structure of the sample but contacted the upper silicone oil layer. Due to the coated oil layer on micro-nano structures, the fecal simulant could not adhere to the PTFE surface. Among six parameters, surface T3 showed the best fecalphobicity.

Adhesion property can be predicted by adhesion work described by Eq. (5), where R is surface roughness; γ is interfacial energy between surface 1/2/3 and 1/2/3 means solid substrate/oil layer/air.

$$w_a = R(\gamma_{13} \times \gamma_{23})^{1/2} \quad (5)$$

After laser ablation, roughness increased the adhesion force significantly compared to the non-processed PTFE (Table S6). However, after coating with the oil, all samples' adhesion tended to be the same. The adhesion work decreased 46 % compared with non-processed PTFE and at least 87 % with laser-ablated PTFE. After oil coating, surface roughness approached lower, so fecal simulant could slide out of the surface with silicone oil coating but stick on the laser-ablated PTFE surface.

In general, it can be predicted that a higher adhesion force can lead to a higher friction force [58], and the adhesion work can influence the velocity-dependent property of micro friction force [59]. Israelachvili's group found that friction and adhesion forces can be highly correlated in similar experimental conditions [58]. When the fecal simulant fell on the sample surface, the simulant would slide off due to its own gravity and the friction of the surface, as shown in Fig. 4d. As Fig. 4d presented, the silicone oil coating will reduce the μ of the sample so that the fecal simulant can slide down easily after the oil coating and would stick on the surface only after the laser ablation due to the μ increase (μ is the friction coefficient of the sample). The machine was also used to measure the friction coefficient of the sample, which showed the same result as the work adhesion calculation. For the non-processed PTFE, the friction coefficient was 0.339, and after laser processing, the friction coefficient increased to 0.434. Therefore, the fecal simulant would adhere to the surface after laser processing after the test. What's more, with the silicone oil's help, the friction coefficient on our fecalphobic sample decreased to 0.289, which indicated that silicone oil has a positive influence on reducing the adhesion of the sample.

3.4. Sanitation application

Conventional toilets require plenty of water to remove urine and feces. For example, a flush-type toilet requires approximately 6000 ml per flush. However, a new latrine toilet combined with a urine-feces separator and a fecalphobic trap door can minimize this. A visualized 3D model design of our toilet prototype, which incorporated a urine-feces separator and an automatic trap door at different views, was shown in Fig. 5a. The Red rectangular was the urine separation part, and the yellow rectangular was the feces separation part with the trap door component, where the tested surfaces would be glued. What's more, a toilet prototype was produced using a weight balance mechanism on its trapdoor (Fig. 5b). The trapdoor closes the bottom hole of the toilet due to the weight balance between the two sides ($w_1 = w_1$). When fecal simulant with a weight of w_2 is dropped, the trap door will open itself due to the weight balance change. When the simulant leaves the surface, the door will automatically close, which means that the trapdoor will automatically open or close with the appearances or disappearances of gravity forces from the simulant's weights (Fig. 5c). This can remove odor from the pit compared to a typical pit-latrine toilet.

The impacts of fecal simulant on the toilet prototype were performed (Fig. 5d, Videos S3, 4). When the simulant was dropped on surface P0, the simulant slowly slid off the surface in 14 s under the simulant's gravity force. Although only a small amount of the simulant was stuck on P0 in the test with 5 g of simulant, 150 g of simulant adhered and stuck on P0. The investigated amount is one-third of the produced daily average of human feces. Therefore, non-processed PTFE cannot apply to existing toilet systems. Among the investigated surfaces, P3 showed the worst result. Fecal simulant immediately stuck on the surface because of the destruction of the air layer and increased adhesion. Due to the large mass of fecal simulant and laminar flow effect, the upper layer of simulant slid down the surface under the action of gravity. In contrast, the lower layer of simulant destroyed the air layer when falling on P3 and adhered to the structure, which was more difficult to slide off. Nevertheless, the simulant slid off from T3 smoothly under the aid of silicone oil in 5 s. The simulant slid down under the silicone oil lubricant and gravity without damaging the sample structure. The impacts of fecal simulant on the investigated surfaces have the same phenomenon as in the test of solid repellency at small simulant weights. Depending on the simulant's weight, the sliding speed on the fecalphobic surface is faster than the non-processed PTFE, with different values from 3 t to 26 times when the simulant's weight reduces from 150 g to 5 g. In the practical uses, the longer time human feces slide on the surface, the higher transmission possibility bacterias and viruses cause. Moreover, the short sliding time and the closure mechanism of the trap door can minimize uncomfortable odors under the ambient air because the feces will be slid off quickly to the pit or container (Fig. 5e).

Supplementary material related to this article can be found online at doi:10.1016/j.colsurfa.2022.130742.

On the other hand, 150 g of the simulant was randomly dropped 30 times on the non-processed PTFE (P0) and the silicone oil coating laser-ablated PTFE (T3) to investigate the amount of necessary water to remove the remaining simulants (Fig. 5f and Table S7). The fecalphobic required no water to clean the simulants in the first four cycles, while P0 required 3137.8 ml of water. When the cycle increases, the silicone oil may be removed under the strong impact of the simulants and slide off the surface with the simulant. As a result, a small amount of the simulants could be stuck on the surface, which needed water to clean. However, after 30 cycles, an average amount of required water, approximately 865.5 ml per time, was used to clean the surface. The required amount was reduced four times more on the fecalphobic surface than on the non-processed one. Compared to a flush-type toilet, the needed water might be less. Moreover, a commercial silicated-based ceramic material, which was always used for conventional sanitation systems, needed three times the required amount of water more than our fecalphobic surface. Also, a commercial white PP material cost about 3.2 times more than our fecalphobic surface (Table S8). This proved that our fecalphobic surfaces could be applied in latrine toilet systems to repel human wastes and reduce water usage (Fig. 5g). Keeping in view of fecalphobic performance and our pit-latrine toilet design, we look forward to a whole sanitation model (Fig. 5e). The urine diverter supports separating human urine and solid wastes while the rainwater can be collected through the rain collection approach [60,61]. The fecalphobic surface installed on the trap door minimizes the use of water and energy to remove human solid wastes. As a proof-of-concept application, the

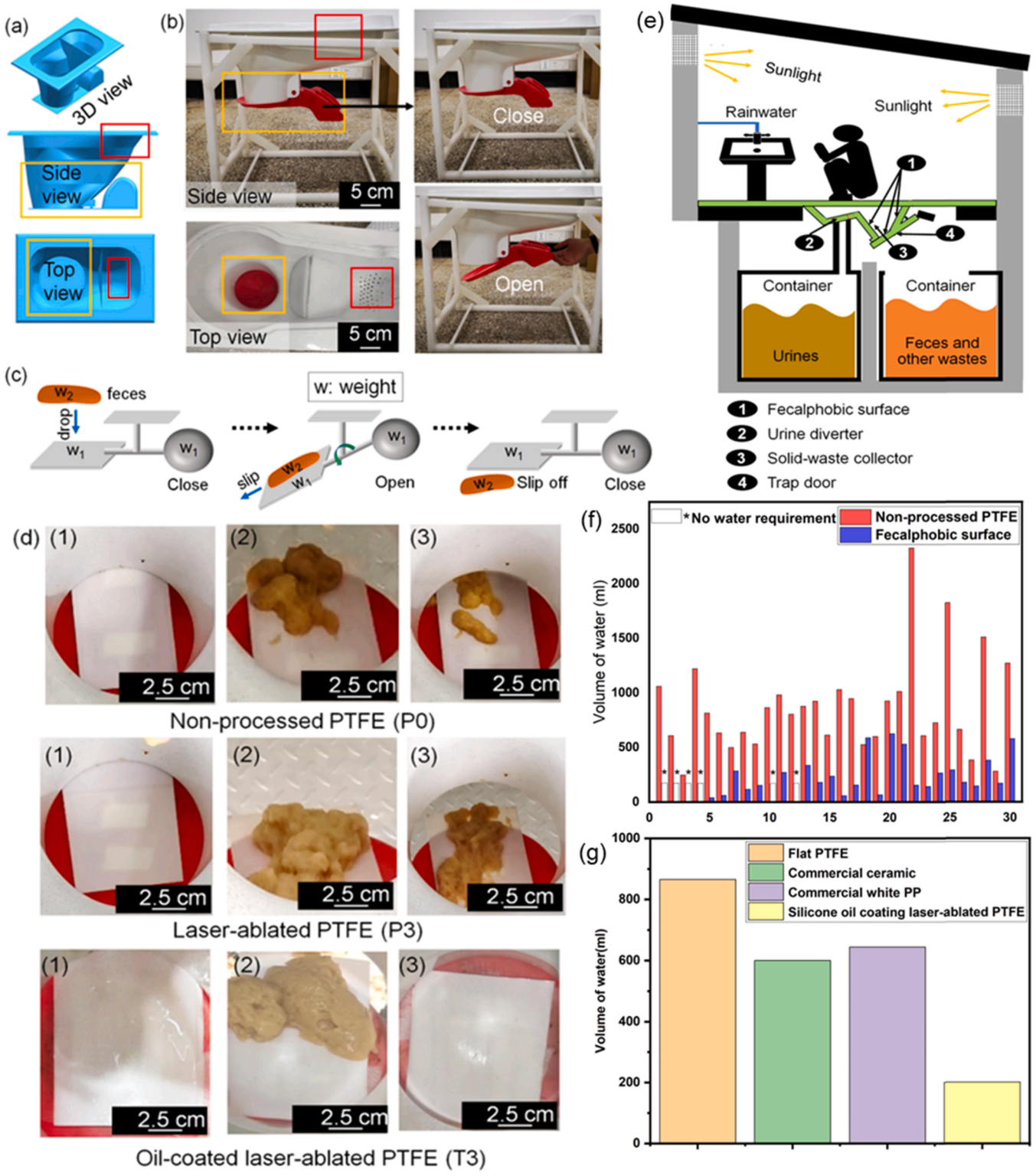

Fig. 5. New pit-latrine toilet and its initial performance for sanitation applications. (a) The 3D model design of our toilet prototype incorporated a urine-feces separator and an automatic trap door at different views. (b) The toilet prototype's side view and top view integrated a urine-feces separator and an automatic trapdoor (before installing a large-size fecalphobic surface on the top), respectively. (c) The working principle of the trap door. (d) Feces-surface interaction test on samples P0, P3, and T3, which were installed on the top of the trapdoor surface. (e) An application model of our pit-latrine toilet concept integrated the fecalphobic surface. (f) The amount of water cleaning the fecal simulants on the non-processed PTFE (P0) and the fecalphobic surface (T3); (g) Comparison of water consumption of clean fecal simulants with different materials.

model can combine various functional surfaces to form a safe, energy-saving, and non-sewered sanitation system.

4. Conclusion

We produced fecalphobic surfaces using a femtosecond laser combined with a silicone oil coating. The femtosecond laser processing creates micro-nano structures, increasing the storage capacity of silicone oil. Additionally, the presence of silicone oil reduces feces' adhesion to the surface. Therefore, various liquids and fecal simulants are slid off the fecalphobic surfaces without using any external water or a small amount of water. The sliding time on the fecalphobic surface is quicker from 3 t to 26 times than on the flat surface when the simulant's weight delines from 150 g to 5 g. In addition, the sliding mechanism is explained due to the low adhesion of the oil layer. A new toilet prototype integrating a urine-feces separator and an automatic trap door is introduced to enhance sanitation quality.

CRediT authorship contribution statement

Yu Liu: Methodology, Investigation, Formal analysis, Writing – original draft; **Gan Yuan:** Investigation; **Fei Xie:** Investigation; **Yang An:** Investigation, Methodology; **Jianwen Sun:** Investigation; **Ning Zhao:** Investigation; **Yongbo Deng:** Investigation; **Longnan Li:** Investigation; **Subhash C. Singh:** Methodology; **Chi-Vinh Ngo:** Conceptualization, Methodology, Formal analysis, Validation, Funding acquisition, Writing – review & editing, Supervision; **Wei Li:** Funding acquisition, Resourses, Writing – review & editing, Supervision; **Chunlei Guo:** Original conceptualization and project definition, Conceptualization, Formal Analysis, Methodology, Validation, Funding acquisition, Resourses, Writing – review & editing, Supervision.

Declaration of Competing Interest

The authors declare that they have no known competing financial interests or personal relationships that could have appeared to influence the work reported in this paper.

Data Availability

Data can be made available upon reasonable requests.

2Acknowledgements

This work was supported by the Bill & Melinda Gates Foundation (INV-009181), National Natural Science Foundation of China (grant nos. 62134009, 62121005), the Innovation Grant of Changchun Institute of Optics, Fine Mechanics and Physics (CIOMP). Jilin Provincial Science and Technology Development Project (grant no. YDZJ202102CXJD002), Chi Vinh Ngo sincerely acknowledges support funded by Chinese Academy of Sciences President's International Fellowship Initiative (Grant No.2022VSB0002).

Appendix A. Supporting information

Supplementary data associated with this article can be found in the online version at doi:10.1016/j.colsurfa.2022.130742.

References

[1] W.H. Organization, State of the world's sanitation: an urgent call to transform sanitation for better health, environments, economies and societies, UNICEF, 2020.
[2] J. Colón, A.A. Forbis-Stokes, M.A. Deshusses, Anaerobic digestion of undiluted simulant human excreta for sanitation and energy recovery in less-developed countries, Energy Sustain. Dev. 29 (2015) 57–64, https://doi.org/10.1016/j.esd.2015.09.005.
[3] W.H. Organization, Progress on household drinking water, sanitation and hygiene 2000–2020: five years into the SDGs, (2021).
[4] K. Ravindra, K.R. Smith, Better kitchens and toilets: both needed for better health, Environ. Sci. Pollut. Res Int 25 (2018) 12299–12302, https://doi.org/10.1007/s11356-018-1879-4.
[5] A. Ilango, O. Lefebvre, Characterizing properties of biochar produced from simulated human feces and its potential applications, J. Environ. Qual. 45 (2016) 734–742, https://doi.org/10.2134/jeq2015.07.0397.
[6] C. Rose, A. Parker, B. Jefferson, E. Cartmell, The characterization of feces and urine: a review of the literature to inform advanced treatment technology, Crit. Rev. Environ. Sci. Technol. 45 (2015) 1827–1879, https://doi.org/10.1080/10643389.2014.1000761.
[7] C. Leong, Narratives of sanitation: motivating toilet use in India, Geoforum 111 (2020) 24–38, https://doi.org/10.1016/j.geoforum.2019.10.001.
[8] K. O'Reilly, E. Louis, The toilet tripod: understanding successful sanitation in rural India, Health Place 29 (2014) 43–51, https://doi.org/10.1016/j.healthplace.2014.05.007.
[9] C.M. Welling, S. Varigala, S. Krishnaswamy, A. Raj, B. Lynch, J.R. Piascik, B. R. Stoner, B.T. Hawkins, M. Hegarty-Craver, M.J. Luettgen, S. Grego, Resolving the relative contributions of cistern and pour flushing to toilet water usage: measurements from urban test sites in India, Sci. Total Environ. 730 (2020), 138957, https://doi.org/10.1016/j.scitotenv.2020.138957.
[10] B. Augsburg, P. Rodríguez-Lesmes, Sanitation dynamics: toilet acquisition and its economic and social implications in rural and urban contexts, J. Water, Sanit. Hyg. Dev. 10 (2020) 628–641, https://doi.org/10.2166/washdev.2020.098.
[11] V.G. Gude, N. Nirmalakhandan, Desalination at low temperatures and low pressures, Desalination 244 (2009) 239–247, https://doi.org/10.1016/j.desal.2008.06.005.
[12] V.G. Gude, Desalination and water reuse to address global water scarcity, Rev. Environ. Sci. Bio-Technol. 16 (2017) 591–609, https://doi.org/10.1007/s11157-017-9449-7.
[13] E. Reynaert, E.E. Greenwood, B. Ndwandwe, M.E. Riechmann, R.C. Sindall, K. M. Udert, E. Morgenroth, Practical implementation of true on-site water recycling systems for hand washing and toilet flushing, Water Res X 7 (2020), 100051, https://doi.org/10.1016/j.wroa.2020.100051.
[14] E.J.M. Blokker, E.J. Pieterse-Quirijns, J.H.G. Vreeburg, J.C. Van Dijk, Simulating Nonresidential Water Demand with a Stochastic End-Use Model, J Water Res Pl-Asce 137 (2011) 511–520, https://doi.org/10.1061/(Asce)Wr.1943-5452.0000146.
[15] C. Rodrigues, J. Almeida, M.I. Santos, A. Costa, S. Além, E. Rufo, A. Tadeu, F. Freire, Environmental Life-Cycle assessment of an innovative multifunctional toilet, Energies 14 (2021), https://doi.org/10.3390/en14082307.
[16] J. Gundlach, M. Bryla, T.A. Larsen, L. Kristoferitsch, H. Gründl, M. Holzner, Novel NoMix toilet concept for efficient separation of urine and feces and its design optimization using computational fluid mechanics, J. Build. Eng. 33 (2021), https://doi.org/10.1016/j.jobe.2020.101500.
[17] S. Zuo, X. Zhou, Z. Li, X. Wang, L. Yu, Investigation on recycling dry toilet generated blackwater by anaerobic digestion: from energy recovery to sanitation, Sustainability 13 (2021), https://doi.org/10.3390/su13084090.
[18] S.C. Singh, M. ElKabbash, Z. Li, X. Li, B. Regmi, M. Madsen, S.A. Jalil, Z. Zhan, J. Zhang, C. Guo, Solar-trackable super-wicking black metal panel for photothermal water sanitation, Nat. Sustain. 3 (2020) 938–946, https://doi.org/10.1038/s41893-020-0566-x.
[19] L. Gao, S. Yang, H. Yang, T. Ma, One-stage method for fabricating superhydrophobic stainless steel surface and its anti-corrosion performance, Adv. Eng. Mater. 19 (2017), https://doi.org/10.1002/adem.201600511.
[20] Y. Liu, G. Yuan, C. Guo, C.-V. Ngo, W. Li, Femtosecond laser fabrication and chemical coating of anti-corrosion ethylene-glycol repellent aluminum surfaces, Mater. Lett. 323 (2022), https://doi.org/10.1016/j.matlet.2022.132562.
[21] A. Gaddam, H. Sharma, T. Karkantonis, S. Dimov, Anti-icing properties of femtosecond laser-induced nano and multiscale topographies, Appl. Surf. Sci. 552 (2021), https://doi.org/10.1016/j.apsusc.2021.149443.
[22] D.K. Chu, S.C. Singh, J.L. Yong, Z.B. Zhan, X.Y. Sun, J.A. Duan, C.L. Guo, Superamphiphobic surfaces with controllable adhesion fabricated by femtosecond laser bessel beam on PTFE, Adv. Mater. Interfaces 6 (2019), 1900550-1900550. https://doi.org/ARTN 190055010.1002/admi.201900550.
[23] X. Gao, J. Zhou, R. Du, Z. Xie, S. Deng, R. Liu, Z. Liu, J. Zhang, Robust superhydrophobic foam: a graphdiyne-based hierarchical architecture for oil/water separation, Adv. Mater. 28 (2016) 168–173, https://doi.org/10.1002/adma.201504407.
[24] F. Li, W. Kong, X. Zhao, Y. Pan, Multifunctional TiO2-based superoleophobic/superhydrophilic coating for oil-water separation and oil purification, ACS Appl. Mater. Interfaces 12 (2020) 18074–18083, https://doi.org/10.1021/acsami.9b22625.
[25] C.-V. Ngo, D.-M. Chun, Effect of heat treatment temperature on the wettability transition from hydrophilic to superhydrophobic on laser-ablated metallic surfaces, Adv. Eng. Mater. 20 (2018), https://doi.org/10.1002/adem.201701086.
[26] J.L. Song, Z.A. Liu, X.Y. Wang, H. Liu, Y. Lu, X. Deng, C.J. Carmalt, I.P. Parkin, High-efficiency bubble transportation in an aqueous environment on a serial wedge-shaped wettability pattern, J. Mater. Chem. A 7 (2019) 13567–13576, https://doi.org/10.1039/c9ta02095k.
[27] Z.A. Liu, H. Liu, W. Li, J.L. Song, Optimization of bioinspired surfaces with enhanced water transportation capacity, Chem. Eng. J. 433 (2022) 9, https://doi.org/10.1016/j.cej.2022.134568.
[28] Z.A. Liu, H. Zhang, Y.Q. Han, L. Huang, Y. Chen, J.Y. Liu, X.Y. Wang, X. Liu, S. Y. Ling, Superaerophilic wedge-shaped channels with precovered air film for

efficient subaqueous bubbles/jet transportation and continuous oxygen supplementation, Acs Appl. Mater. Interfaces 11 (2019) 23808–23814, https://doi.org/10.1021/acsami.9b08085.
[29] S.A. Jalil, M. Akram, J.A. Bhat, J.J. Hayes, S.C. Singh, M. ElKabbash, C. Guo, Creating superhydrophobic and antibacterial surfaces on gold by femtosecond laser pulses, Appl. Surf. Sci. 506 (2020), 144952, https://doi.org/10.1016/j.apsusc.2019.144952.
[30] V.K. Manivasagam, G. Perumal, H.S. Arora, K.C. Popat, Enhanced antibacterial properties on superhydrophobic micro-nano structured titanium surface, J. Biomed. Mater. Res A 110 (2022) 1314–1328, https://doi.org/10.1002/jbm.a.37375.
[31] A.Y. Vorobyev, C.L. Guo, Multifunctional surfaces produced by femtosecond laser pulses, J. Appl. Phys. 117 (2015) https://doi.org/Artn 03310310.1063/1.4905616.
[32] M. Liu, S. Wang, L. Jiang, Nature-inspired superwettability systems, Nat. Rev. Mater. 2 (2017), https://doi.org/10.1038/natrevmats.2017.36.
[33] B. Su, Y. Tian, L. Jiang, Bioinspired interfaces with superwettability: from materials to chemistry, J. Am. Chem. Soc. 138 (2016) 1727–1748, https://doi.org/10.1021/jacs.5b12728.
[34] J.L. Yong, F. Chen, Q. Yang, Y. Fang, J.L. Huo, J.Z. Zhang, X. Hou, Nepenthes inspired design of self-repairing omniphobic slippery liquid infused porous surface (SLIPS) by femtosecond laser direct writing, Adv. Mater. Interfaces 4 (2017) https://doi.org/ARTN 170055210.1002/admi.201700552.
[35] X. Lv, Y. Jiao, S. Wu, C. Li, Y. Zhang, J. Li, Y. Hu, D. Wu, Anisotropic sliding of underwater bubbles on microgrooved slippery surfaces by one-step femtosecond laser Scanning, ACS Appl. Mater. Interfaces 11 (2019) 20574–20580, https://doi.org/10.1021/acsami.9b06849.
[36] Y. Fang, J. Yong, Y. Cheng, Q. Yang, X. Hou, F. Chen, Liquid-Infused slippery stainless steel surface prepared by alcohol-assisted femtosecond laser ablation, Adv. Mater. Interfaces 8 (2021), https://doi.org/10.1002/admi.202001334.
[37] M.J. Kreder, D. Daniel, A. Tetreault, Z. Cao, B. Lemaire, J.V.I. Timonen, J. Aizenberg, Film dynamics and lubricant depletion by droplets moving on lubricated surfaces, Phys. Rev. X 8 (2018), https://doi.org/10.1103/PhysRevX.8.031053.
[38] H. Liu, P. Zhang, M. Liu, S. Wang, L. Jiang, Organogel-based thin films for self-cleaning on various surfaces, Adv. Mater. 25 (2013) 4477–4481, https://doi.org/10.1002/adma.201301289.
[39] Y. Long, X. Yin, P. Mu, Q. Wang, J. Hu, J. Li, Slippery liquid-infused porous surface (SLIPS) with superior liquid repellency, anti-corrosion, anti-icing and intensified durability for protecting substrates, Chem. Eng. J. 401 (2020), https://doi.org/10.1016/j.cej.2020.126137.
[40] J. Liang, H. Bian, Q. Yang, Y. Fang, C. Shan, X. Bai, Y. Cheng, J.L. Yong, X. Hou, F. Chen, Femtosecond laser-patterned slippery surfaces on PET for liquid patterning and blood resistance, Opt. Laser Technol. 132 (2020). .https://doi.org/ARTN 10646910.1016/j.optlastec.2020.106469.
[41] G. Verma, G. Yadav, C.S. Saraj, L. Li, N. Miljkovic, J.P. Delville, W. Li, A versatile interferometric technique for probing the thermophysical properties of complex fluids, Light Sci. Appl. 11 (2022) 115, https://doi.org/10.1038/s41377-022-00796-7.
[42] J. Wang, L. Wang, N. Sun, R. Tierney, H. Li, M. Corsetti, L. Williams, P.K. Wong, T. S. Wong, Viscoelastic solid-repellent coatings for extreme water saving and global sanitation, Nat. Sustain. 2 (2019) 1097–1105, https://doi.org/10.1038/s41893-019-0421-0.
[43] R. Penn, B.J. Ward, L. Strande, M. Maurer, Review of synthetic human faeces and faecal sludge for sanitation and wastewater research, Water Res 132 (2018) 222–240, https://doi.org/10.1016/j.watres.2017.12.063.
[44] R. Penn, M. Maurer, F.G. Michalec, A. Scheidegger, J. Zhou, M. Holzner, Quantifying physical disintegration of faeces in sewers: stochastic model and flow reactor experiments, Water Res 152 (2019) 159–170, https://doi.org/10.1016/j.watres.2018.12.037.
[45] M. Xi, J. Yong, F. Chen, Q. Yang, X. Hou, A femtosecond laser-induced superhygrophobic surface: beyond superhydrophobicity and repelling various complex liquids, RSC Adv. 9 (2019) 6650–6657, https://doi.org/10.1039/c8ra08328b.
[46] T.S. Wong, S.H. Kang, S.K. Tang, E.J. Smythe, B.D. Hatton, A. Grinthal, J. Aizenberg, Bioinspired self-repairing slippery surfaces with pressure-stable omniphobicity, Nature 477 (2011) 443–447, https://doi.org/10.1038/nature10447.
[47] D.J. Preston, Y. Song, Z. Lu, D.S. Antao, E.N. Wang, Design of lubricant infused surfaces, ACS Appl. Mater. Interfaces 9 (2017) 42383–42392, https://doi.org/10.1021/acsami.7b14311.
[48] J.N. Israelachvili, Intermol. Surf. Forces (2011).
[49] D. Daniel, J.V.I. Timonen, R.P. Li, S.J. Velling, J. Aizenberg, Oleoplaning droplets on lubricated surfaces, 1020-+, Nat. Phys. 13 (2017) https://doi.org/10.1038/Nphys4177.
[50] J.D. Smith, R. Dhiman, S. Anand, E. Reza-Garduno, R.E. Cohen, G.H. McKinley, K. K. Varanasi, Droplet mobility on lubricant-impregnated surfaces, Soft Matter 9 (2013) 1772–1780, https://doi.org/10.1039/c2sm27032c.
[51] A.B.D. Cassie, S. Baxter, Wettability of porous surfaces, T Faraday Soc. 40 (1944) 0546–0550, https://doi.org/DOI 10.1039/tf9444000546.
[52] R.N. Wenzel, Resistance of solid surfaces to wetting by water, Ind. Eng. Chem. 28 (1936) 988–994, https://doi.org/DOI 10.1021/ie50320a024.
[53] J. Liang, C. Shan, H. Wang, T. Hu, Q. Yang, H.Y. Li, X. Hou, F. Chen, Highly stable and transparent slippery surface on silica glass fabricated by femtosecond laser, Adv. Eng. Mater. 24 (2022) 7, https://doi.org/10.1002/adem.202200708.
[54] S. Kim, T. Wang, L. Zhang, Y. Jiang, Droplet impacting dynamics on wettable, rough and slippery oil-infuse surfaces, J. Mech. Sci. Technol. 34 (2020) 219–228, https://doi.org/10.1007/s12206-019-1223-z.
[55] Y.Z. Shen, H.J. Tao, S.L. Chen, Y.J. Xie, T. Zhou, T. Wang, J. Tao, Water repellency of hierarchical superhydrophobic Ti6Al4V surfaces improved by secondary nanostructures, Appl. Surf. Sci. 321 (2014) 469–474, https://doi.org/10.1016/j.apsusc.2014.10.044.
[56] C. Hao, J. Li, Y. Liu, X. Zhou, Y. Liu, R. Liu, L. Che, W. Zhou, D. Sun, L. Li, L. Xu, Z. Wang, Superhydrophobic-like tunable droplet bouncing on slippery liquid interfaces, Nat. Commun. 6 (2015) 7986, https://doi.org/10.1038/ncomms8986.
[57] P. Gregorčič, B. Šetina-Batič, M. Hočevar, Controlling the stainless steel surface wettability by nanosecond direct laser texturing at high fluences, Appl. Phys. A 123 (2017), https://doi.org/10.1007/s00339-017-1392-5.
[58] J.N. Israelachvili, Y.L. Chen, H. Yoshizawa, Relationship between adhesion and friction forces, J. Adhes. Sci. Technol. 8 (1994) 1231–1249, https://doi.org/Doi 10.1163/156856194×00582.
[59] X.J. Zhang, Y.K. Dong, Y.G. Meng, S.Z. Wen, Investigation on adhesion work and its effects on micro friction, Adv. Mach. Manuf. Technol. Viii 315–316 (2006) 784–787, https://doi.org/DOI 10.4028/www.scientific.net/KEM.315-316.784.
[60] G. Yuan, Y. Liu, F. Xie, C. Guo, C.V. Ngo, W. Li, Fabrication of superhydrophobic gully-structured surfaces by femtosecond laser and imprinting for high-efficiency self-cleaning Rain collection, Langmuir 38 (2022) 2720–2728, https://doi.org/10.1021/acs.langmuir.1c03488.
[61] J. Lu, C.V. Ngo, S.C. Singh, J. Yang, W. Xin, Z. Yu, C. Guo, Bioinspired hierarchical surfaces fabricated by femtosecond laser and hydrothermal method for water harvesting, Langmuir 35 (2019) 3562–3567, https://doi.org/10.1021/acs.langmuir.8b04295.